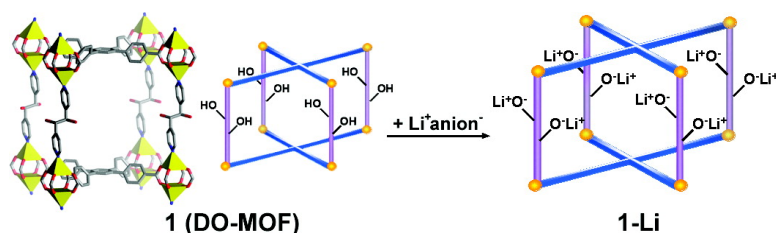


## Post-Synthesis Alkoxide Formation Within Metal/Organic Framework Materials: A Strategy for Incorporating Highly Coordinatively Unsaturated Metal Ions

Karen L. Mulfort, Omar K. Farha, Charlotte L. Stern, Amy A. Sarjeant, and Joseph T. Hupp  
*J. Am. Chem. Soc.*, **2009**, 131 (11), 3866-3868 • DOI: 10.1021/ja809954r • Publication Date (Web): 26 February 2009

Downloaded from <http://pubs.acs.org> on March 30, 2009



### More About This Article

Additional resources and features associated with this article are available within the HTML version:

- Supporting Information
- Access to high resolution figures
- Links to articles and content related to this article
- Copyright permission to reproduce figures and/or text from this article

[View the Full Text HTML](#)

## Post-Synthesis Alkoxide Formation Within Metal–Organic Framework Materials: A Strategy for Incorporating Highly Coordinatively Unsaturated Metal Ions

Karen L. Mulfort,<sup>†,‡</sup> Omar K. Farha,<sup>†</sup> Charlotte L. Stern,<sup>†</sup> Amy A. Sarjeant,<sup>†</sup> and Joseph T. Hupp<sup>\*,†</sup>

*Department of Chemistry, Northwestern University, 2145 Sheridan Road, Evanston, Illinois 60208, and Division of Chemical Sciences and Engineering, Argonne National Laboratory, Argonne, Illinois 60439*

Received December 21, 2008; E-mail: j-hupp@northwestern.edu

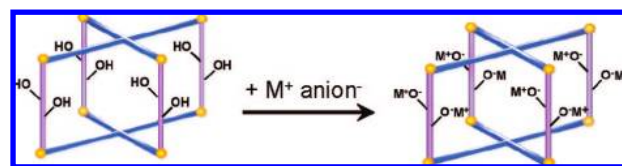
Metal–organic framework (MOF) materials have received considerable attention as potential high-performance, multifunctional molecular sorbents.<sup>1</sup> The attention derives in part from their typically very high internal surface areas, low densities, and permanent microporosity. Also highly attractive is their (typically) crystalline nature, a characteristic that ensures complete uniformity of channel sizes (for a given MOF) and allows one to determine the position of every atom composing the framework. In turn, the detailed positional information allows for high-quality computational modeling of observed or anticipated sorption behavior. Additionally, the hybrid nature of the materials facilitates immense structural and chemical variety. Taken together, these features point to the opportunity to initially design (and/or modify after synthesis<sup>2</sup>) the steric and chemical properties of the pores in order to tune host–guest interactions with sufficient precision to render the sorbent materials highly functional for specialized applications such as chemical separations, gas storage, and selective catalysis.

On the basis of both experimental and computational studies, it has become increasingly clear that the presence of coordinatively unsaturated metal centers can greatly enhance the performance of MOFs in the above-mentioned applications.<sup>3</sup> The approaches to introducing accessible metal centers include (a) exploitation of incidental structural defects that leave metal-containing nodes incompletely coordinated,<sup>4</sup> (b) use of metal complexes (porphyrins, salens, etc.) as “organic” struts,<sup>5</sup> (c) electrostatic encapsulation of metal complexes or solvated (or unsolvated<sup>6</sup>) metal cations by anionic frameworks,<sup>7</sup> (d) incorporation of metal-containing nodes featuring thermally removable solvent molecules as ligands,<sup>8</sup> (e) binding of metal salts to reactive sites (e.g., silver nitrate attachment to strut alkyne functionalities),<sup>9</sup> and (f) photochemical attachment of organometallic complexes to aromatic components of struts.<sup>10</sup>

Here we discuss an attractive alternative approach based on conversion of pendant alcohols to metal alkoxides (Scheme 1) and investigate its application to reversible uptake of molecular hydrogen.<sup>11</sup> In contrast to all of the above except (c), the pendant-alcohol strategy readily allows for incorporation of alkali metal ions. Lithium ions in particular have attracted considerable attention in theoretical investigations of MOFs because of their potential for engendering high heats of adsorption for H<sub>2</sub>.<sup>12–15</sup>

We turned to the alkoxide approach after previously exploring chemical reduction of MOF struts as a means of incorporating alkali metal cations.<sup>16</sup> While initial findings were encouraging (e.g., enhancements of H<sub>2</sub> uptake by up to 75%), limitations to the reduction approach subsequently became evident, at least for the MOFs examined. Briefly, it appears that the incorporated cations (a) localize around carboxylates rather than the reduced portions

**Scheme 1.** Metal Alkoxide Formation within a Porous Framework



of the struts<sup>13</sup> and (b) are largely shielded from direct interaction with H<sub>2</sub>, exerting their effects instead by facilitating favorable displacement of catenated frameworks. With these problems in mind, we sought an alternative approach that would avoid catenation and anchor ions far from carboxylates or nodes.

Catenation was addressed by using the recently developed “octa”-oxygen ligand, **L1**.<sup>17</sup> In contrast to most other carboxylate ligands used in pillared-paddlewheel structures, **L1** often yields noncatenated structures. As Figure 1 shows, the combination of **L1** with a Zn(II) source and the diol-containing strut, **L2**, gives, after 2 days of heating, colorless block crystals of **1**, which we have termed **DO-MOF**. Single-crystal X-ray measurements confirmed that **1** consists of only a single network containing large cavities with readily accessible alcohol functionalities. Application of the SQUEEZE routine in PLATON revealed a remarkable 76% solvent-accessible void volume.<sup>18</sup> Characterization by thermal gravimetric

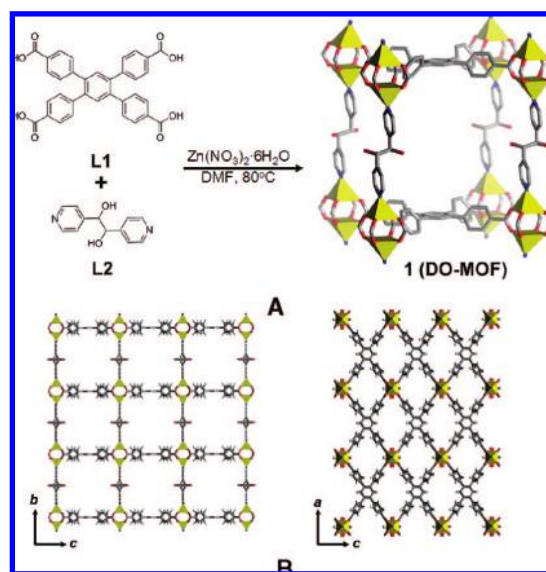


**Figure 1.** (A) Chemical structures of **L1** and **L2** and the crystal structure of **1** (**DO-MOF**). Gray, carbon; blue, nitrogen; red, oxygen; yellow tetrahedra, zinc. Hydrogens and solvent molecules have been omitted for clarity. (B) Packing diagram of **1** down the (left) *a* and (right) *b* axes.

<sup>†</sup> Northwestern University.

<sup>‡</sup> Argonne National Laboratory.

**Table 1.** Summary of Adsorption Properties of **1** and **1-M**

material	M	M/Zn <sub>2</sub> <sup>a</sup>	BET surface area (m <sup>2</sup> /g)	pore volume (cm <sup>3</sup> /g) <sup>c</sup>	H <sub>2</sub> uptake (wt %) at 1 atm, 77 K	Q <sub>st</sub> (kJ/mol) at 0–1 atm	solvent/M <sup>e</sup>
<b>1</b> (DO-MOF)	H <sup>+</sup>	2 <sup>b</sup>	810	0.35	1.23	6.3–4.7	n/a
<b>1-Li</b> <sub>0.20</sub>	Li <sup>+</sup>	0.20 ± 0.01	840	0.46	1.32	6.3–6.6	0.40 <sup>f</sup>
<b>1-Li</b> <sub>2.62</sub> <sup>d</sup>	Li <sup>+</sup>	2.62 ± 0.05	270	0.20	0.77	5.6–0.5	0.13 <sup>f</sup>
<b>1-Mg</b> <sub>0.86</sub>	Mg <sup>2+</sup>	0.86 ± 0.02	820	0.40	1.16	6.2–6.9	0.08 <sup>g</sup>
<b>1-Mg</b> <sub>2.02</sub>	Mg <sup>2+</sup>	2.02 ± 0.02	510	0.29	1.01	7.3–5.0	1.10 <sup>h</sup>

<sup>a</sup> Determined via inductively coupled plasma analysis of dissolved samples. <sup>b</sup> From the crystal structure. <sup>c</sup> Measured at  $P/P_0 \approx 0.95$ . <sup>d</sup> Sample showed substantial loss of crystallinity, suggesting degradation. <sup>e</sup> Total number of residual solvent molecules per M atom, as determined by <sup>1</sup>H NMR analysis of the evacuated material (see the SI). <sup>f</sup> DMF + THF. <sup>g</sup> DMF + THF + (methanol or methoxide). <sup>h</sup> 0.19 DMF + 0.04 THF + 0.88 (methanol or methoxide).

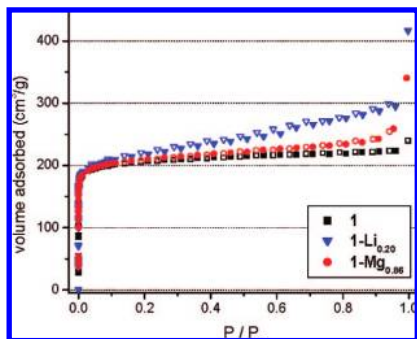


**Figure 2.** N<sub>2</sub> adsorption isotherms of **1**, **1-Li**<sub>0.20</sub>, and **1-Mg**<sub>0.86</sub>. Closed symbols, adsorption; open symbols, desorption.

analysis [see the Supporting Information (SI)] gave a value of 55%. Solvent loss ended at 150 °C, with degradation occurring only above 300 °C. N<sub>2</sub> adsorption (77 K) for the solvent-evacuated version of **1** yielded a type-I isotherm (Figure 2), indicating microporosity, and a BET surface area of 810 m<sup>2</sup>/g<sup>19</sup> (Table 1).

Once we had established the structural stability of this large-pore material, we set out to convert alcohol functionalities to lithium alkoxides. After preliminary experiments indicated that harsh reagents (e.g., methyl lithium) degraded the MOF, we turned to a much milder reagent, lithium *t*-butoxide.<sup>20</sup> Exchange of hydroxyl protons was achieved by replacing (via soaking) the initially present guest solvent molecules (DMF) with more volatile THF molecules and then stirring **DO-MOF** in an excess of Li<sup>+</sup>[O(CH<sub>3</sub>)<sub>3</sub>]<sup>-</sup> in CH<sub>3</sub>CN/THF (see the SI). The extent of lithium loading was controlled by adjusting the stirring rate and time.

Samples of **1-Li** were activated by heating at 200 °C under reduced pressure for 24 h. <sup>1</sup>H NMR (dissolved samples; Table 1) established that activation removes nearly all of the solvent, while N<sub>2</sub> adsorption measurements (Figure 2) showed that **1** remains microporous after lithiation. At low loading [0.20 Li/Zn<sub>2</sub> (**1-Li**<sub>0.20</sub>)], the MOF retains its sizable surface area (Table 1). However, in the extreme of high loading (**1-Li**<sub>2.62</sub>), both the surface area and micropore volume diminish. Additionally, crystallinity is lost. The effects are tentatively ascribed to partial displacement of zinc by lithium, as simple ROH to ROM conversion should limit the Li/Zn<sub>2</sub> ratio to 2. Notably, no unreacted Li<sup>+</sup>[O(CH<sub>3</sub>)<sub>3</sub>]<sup>-</sup> was detected.

As Figure 3 shows, low-pressure adsorption of H<sub>2</sub> by **1** is reversible at 77 K and reaches 1.23 wt % at 1 atm (Table 1). **1-Li**<sub>0.20</sub> exhibits only slightly greater uptake (1.32 wt % at 1 atm). Nevertheless, the increase corresponds to two additional H<sub>2</sub> per Li<sup>+</sup>. This finding is broadly consistent with computational predictions that an exposed lithium cation on carbon or MOF materials can (depending on pressure) directly bind up to six H<sub>2</sub> molecules.<sup>21</sup> Unfortunately, extension of the measurements to the highly lithiated sample (**1-Li**<sub>2.62</sub>) yielded inferior sorption behavior, provisionally ascribed to partial framework degradation.

H<sub>2</sub> uptake was also examined at 87 K. Fits of 77 and 87 K isotherms to a virial equation (see the SI) enabled pressure-dependent isosteric heats of adsorption, Q<sub>st</sub>, to be determined.<sup>22</sup> As Figure 3B shows, unreacted **1** displays more-or-less “typical” MOF behavior, i.e., a modest initial Q<sub>st</sub> value that decreases with increasing H<sub>2</sub> sorption; this is expected if the first molecules to enter the material bind at the sites offering the highest interaction energy. Though the initial value (6.3 kJ/mol) is well below that necessary for practical H<sub>2</sub> storage, on the basis of binding-relevant factors such as pore size, **1** compares well to similarly structured materials.<sup>1d</sup> **1-Li**<sub>0.20</sub> exhibits much more unusual behavior. While the value of Q<sub>st</sub> at very low H<sub>2</sub> loading is similar to that for **1**, it increases at higher H<sub>2</sub> loading. While rare, behavior of this kind has occasionally been described, most notably for a series of Ti(III)-decorated porous silicas.<sup>23</sup> There the observation was rationalized in terms of changes in the mode of binding to Ti(III) with increasing number of hydrogens, with the change facilitated by the ability of Ti(III) to engage in d-orbital-based Kubas interactions with H<sub>2</sub>.<sup>24</sup> In the case of **1-Li**, the metals cannot deploy Kubas binding. Nevertheless, they appear to engender specific interactions that are absent in the parent MOF material.

Reasoning that replacement of Li<sup>+</sup> by a more highly charged cation might increase the heat of adsorption (for example, via greater local field strength<sup>15</sup> or enhancement of charge–quadrupole interactions<sup>14,25</sup>), we also examined Mg<sup>2+</sup>-containing versions of **DO-MOF**. These were prepared by reacting **1** with methanolic solutions of Mg(OMe)<sub>2</sub> and then activating as described above. Materials containing either ~1 or ~2 magnesium ions per glycol strut (**1-Mg**<sub>0.86</sub> or **1-Mg**<sub>2.02</sub>, respectively) were obtained, depending on the reaction conditions (see the SI).

**1-Mg**<sub>0.86</sub> is assumed to contain individual dications that are bound to pairs of **L2** alkoxide oxygens but are otherwise free of ligands, consistent with <sup>1</sup>H NMR data for the dissolved material (Table S2 in the SI). Figure 3A shows that Mg<sup>2+</sup> incorporation has surprisingly little effect on H<sub>2</sub> uptake at 77 K but does alter the binding, eliciting the same unusual increase in Q<sub>st</sub> with H<sub>2</sub> loading as found for **1-Li**. That the absolute Q<sub>st</sub> values are so similar for **1-Mg**<sub>0.86</sub> and **1-Li**<sub>0.20</sub>, however, suggests that the presence of an additional **L2** alkoxide oxygen for Mg<sup>2+</sup> very effectively diminishes the charge and/or field experienced by proximal H<sub>2</sub> molecules.

For the more highly loaded material **1-Mg**<sub>2.02</sub>, we assume that every **L2** alkoxide site binds a dication independently (necessitating a second charge-balancing anion for each Mg<sup>2+</sup>, presumably a methoxide anion). Repeated attempts to obtain single crystals after magnesium functionalization (and thereby confirm the coordination) were unsuccessful. Nevertheless, <sup>1</sup>H NMR characterization of dissolved samples (Table S2 in the SI) is consistent with retention of ~1 methoxide per Mg<sup>2+</sup>.

In contrast to the case of **1-Mg**<sub>0.86</sub>, the N<sub>2</sub>-accessible surface area of **1-Mg**<sub>2.02</sub> is somewhat diminished relative to the parent MOF. The H<sub>2</sub> uptake is also diminished (see Table 1 and the SI), and the

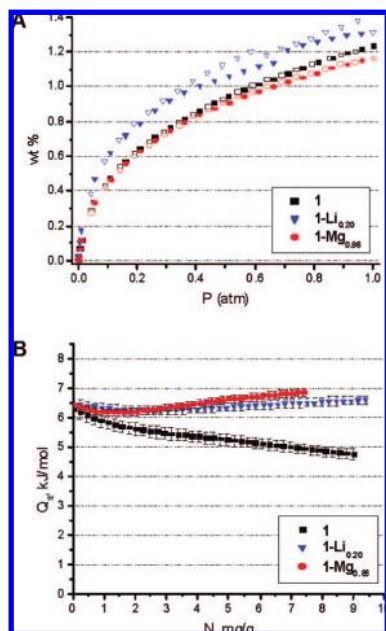


**Figure 3.** (A) Low-pressure  $\text{H}_2$  adsorption isotherms of **1**, **1-Li**<sub>0.20</sub>, and **1-Mg**<sub>0.86</sub>. Closed symbols, adsorption; open symbols, desorption. (B)  $\text{H}_2$  isosteric heats of adsorption of **1**, **1-Li**<sub>0.20</sub>, and **1-Mg**<sub>0.86</sub>.

unusual increase of  $Q_{\text{st}}$  with  $\text{H}_2$  loading is absent in the more highly metalated MOF. Evidently, the presence of ligands other than struts is detrimental to the performance of added metal ions as sorption sites. The appropriate use of diol-containing struts (as opposed to monoalcohols) therefore appears to be an important design consideration when using MOF-based alkoxides to incorporate dications.

In summary, we have introduced a noncatenated hydroxyl-functionalized MOF and exchanged the hydroxyl protons for lithium and magnesium cations via solution methods. At low to intermediate levels of cation substitution, the activated metals appear to be naked, apart from alkoxide (**L2** strut) anchoring, resulting in unusual  $Q_{\text{st}}$  behavior and modest enhancement of  $\text{H}_2$  sorption ( $\sim 2$  additional  $\text{H}_2$  per added  $\text{Li}^+$  at 77 K and 1 atm). While the focus here has been on metal ions that may improve hydrogen sorption, the strategy may well prove to be a general one that is also suitable for metals that facilitate chemical catalysis<sup>11</sup> or separations. We are currently investigating these possibilities as well as continuing investigations of  $\text{H}_2$  sorption.

**Acknowledgment.** We thank Dr. Andy Ott for assistance with crystallography and Patrick Ryan for the calculation of theoretical surface area. We gratefully acknowledge the U.S. Department of Energy (Grant DE-FG02-08-15967) and the Northwestern NSEC for financial support. K.L.M. gratefully acknowledges a Laboratory-Grad Fellowship from Argonne National Laboratory.

**Supporting Information Available:** Full synthesis details for **1**, crystallographic data for **1** in CIF format, preparation details for all **1-M** compounds,  $\text{N}_2$  adsorption isotherms of **1-Li**<sub>2.62</sub> and **1-Mg**<sub>2.02</sub>,  $\text{H}_2$  adsorption isotherms, details of isosteric heat of adsorption calculations, and details of  $^1\text{H}$  NMR analysis of evacuated **1** and **1-M**. This material is available free of charge via the Internet at <http://pubs.acs.org>.

## References

- (1) (a) Férey, G. *Chem. Soc. Rev.* **2008**, *37*, 191–214. (b) Collins, D. J.; Zhou, H.-C. *J. Mater. Chem.* **2007**, *17*, 3154–3160. (c) Lin, X.; Jia, J.; Hubberstey,

- P.; Schroder, M.; Champness, N. R. *CrystEngComm* **2007**, *9*, 438–448. (d) Zhao, D.; Yuan, D.; Zhou, H.-C. *Energy Environ. Sci.* **2008**, *1*, 222–235.
- (2) (a) Gadzikwa, T.; Lu, G.; Stern, C. L.; Wilson, S. R.; Hupp, J. T.; Nguyen, S. T. *Chem. Commun.* **2008**, 5493–5495. (b) Farha, O. K.; Mulfort, K. L.; Hupp, J. T. *Inorg. Chem.* **2008**, *47*, 10223–10225. (c) Wang, Z.; Cohen, S. M. *Angew. Chem., Int. Ed.* **2008**, *47*, 4699–4702. (d) Tanabe, K. K.; Wang, Z.; Cohen, S. M. *J. Am. Chem. Soc.* **2008**, *130*, 8508–8517. (e) Morris, W.; Doonan, C. J.; Furukawa, H.; Banerjee, R.; Yaghi, O. M. *J. Am. Chem. Soc.* **2008**, *130*, 12626–12627. (f) Hwang, Y. K.; Hong, D.-Y.; Chang, J.-S.; Jhung, H.; Seo, Y.-K.; Kim, J.; Vimont, A.; Daturi, M.; Serre, C.; Férey, G. *Angew. Chem., Int. Ed.* **2008**, *47*, 4144–4148.
- (3) (a) Bae, Y.-S.; Farha, O. K.; Spokoyny, A. M.; Mirkin, C. A.; Hupp, J. T.; Snurr, R. Q. *Chem. Commun.* **2008**, 4135–4137. (b) Dinca, M.; Dailly, A.; Liu, Y.; Brown, C. M.; Neumann, D. A.; Long, J. R. *J. Am. Chem. Soc.* **2006**, *128*, 16876–16883. (c) Chen, B.; Ockwig, N. W.; Millward, A. R.; Contreras, D. S.; Yaghi, O. M. *Angew. Chem., Int. Ed.* **2005**, *44*, 4745–4749. (d) Dinca, M.; Long, J. R. *Angew. Chem., Int. Ed.* **2008**, *47*, 6766–6779.
- (4) Fujita, M.; Kwon, Y. J.; Washizu, S.; Ogura, K. *J. Am. Chem. Soc.* **1994**, *116*, 1151–1152.
- (5) (a) Cho, S.-H.; Ma, B.; Nguyen, S. T.; Hupp, J. T.; Albrecht-Schmitt, T. E. *Chem. Commun.* **2006**, 2563–2565. (b) Chen, B.; Zhao, X.; Putkham, A.; Hong, K.; Lobkovsky, E. B.; Hurtado, E. J.; Fletcher, A. J.; Thomas, K. M. *J. Am. Chem. Soc.* **2008**, *130*, 6411–6423. (c) Smithenry, D. W.; Wilson, S. R.; Suslick, K. S. *Inorg. Chem.* **2003**, *42*, 7719–7721.
- (6) Yang, S.; Lin, X.; Blake, A. J.; Thomas, K. M.; Hubberstey, P.; Champness, N. R.; Schroder, M. *Chem. Commun.* **2008**, 6108–6110.
- (7) (a) Liu, Y.; Kravtsov, V. C.; Larsen, R.; Eddaoudi, M. *Chem. Commun.* **2006**, 1488–1490. (b) Alkordi, M. H.; Liu, Y.; Larsen, R. W.; Eubank, J. F.; Eddaoudi, M. *J. Am. Chem. Soc.* **2008**, *130*, 12639–12641. (c) Liu, Y.; Kravtsov, V. C.; Eddaoudi, M. *Angew. Chem., Int. Ed.* **2008**, *47*, 8446–8449.
- (8) In some cases, alteration of the chemical identity of node-localized metal ions has proven feasible via cation exchange. For example, see: Dinca, M.; Long, J. R. *J. Am. Chem. Soc.* **2007**, *129*, 11172–11176.
- (9) Emberger, G. A.; Bae, Y.-S.; Nguyen, S. T.; Hupp, J. T.; Broadbelt, L. J.; Snurr, R. Q. In *Proceedings of the 8th International Conference on Characterization of Porous Solids (COPS VIII)*, Edinburgh, U.K., June 10–13, 2008.
- (10) Kaye, S. S.; Long, J. R. *J. Am. Chem. Soc.* **2008**, *130*, 806–807.
- (11) A precedent of sorts should be noted: Wu, C.-D.; Hu, A.; Zhang, L.; Lin, W. *J. Am. Chem. Soc.* **2005**, *127*, 8940–8941. These authors used binaphthanol-containing structures to immobilize catalytic Ti(IV) centers and accompanying charge-compensating ligands. For condensed-phase catalysis, charge-compensating species present little difficulty since they may dissociate from the active site. For gas sorption, on the other hand, our experience has been that these “extra” species inhibit the interaction of sorbates with metal centers.<sup>9</sup> Additionally, while our work was in progress, a computational study of  $\text{H}_2$  binding by a (hypothetical) lithium alkoxide-containing MOF appeared<sup>15</sup>.
- (12) (a) Han, S. S.; Goddard, W. A., III. *J. Am. Chem. Soc.* **2007**, *129*, 8422–8423. (b) Blomqvist, A.; Araujo, C. M.; Srepusharawoot, P.; Ahuja, R. *Proc. Natl. Acad. Sci. U.S.A.* **2007**, *104*, 20173–20176.
- (13) Dalach, P.; Frost, H.; Snurr, R. Q.; Ellis, D. E. *J. Phys. Chem. C* **2008**, *112*, 9278–9284.
- (14) Belof, J. L.; Stern, A. C.; Eddaoudi, M.; Space, B. *J. Am. Chem. Soc.* **2007**, *129*, 15202–15210.
- (15) Klontzas, E.; Mavrandonakis, A.; Tylianakis, E.; Froudakis, G. E. *Nano Lett.* **2008**, *8*, 1572–1576.
- (16) (a) Mulfort, K. L.; Hupp, J. T. *J. Am. Chem. Soc.* **2007**, *129*, 9604–9605. (b) Mulfort, K. L.; Hupp, J. T. *Inorg. Chem.* **2008**, *47*, 7936–7938. (c) Mulfort, K. L.; Wilson, T. M.; Wasielewski, M. R.; Hupp, J. T. *Langmuir* **2009**, *25*, 503–508.
- (17) Farha, O. K.; Mulfort, K. L.; Hupp, J. T. *Inorg. Chem.* **2008**, *47*, 10223–10225.
- (18) Spek, A. L. *J. Appl. Crystallogr.* **2003**, *36*, 7–13.
- (19) Notably, the calculated maximum  $\text{N}_2$ -accessible surface area is 4000  $\text{m}^2/\text{g}$ . The disparity between this and the experimental value of  $\sim 800$   $\text{m}^2/\text{g}$  presumably is a reflection of either partial channel collapse or pore blockage at particle–particle interfaces.
- (20) Hanna, T. A.; Liu, L.; Angeles-Boza, A. M.; Kou, X.; Gutsche, C. D.; Ejsmont, K.; Watson, W. H.; Zakharov, L. N.; Incarvito, C. D.; Rheingold, A. L. *J. Am. Chem. Soc.* **2003**, *125*, 6228–6238.
- (21) Barbatti, M.; Jalbert, G.; Nascimento, M. A. C. *J. Chem. Phys.* **2001**, *114*, 2213–2218.
- (22) Czepirski, L.; Jagiello, J. *Chem. Eng. Sci.* **1989**, *44*, 797–801.
- (23) (a) Hu, X.; Skadchenko, B. O.; Trudeau, M.; Antonelli, D. M. *J. Am. Chem. Soc.* **2006**, *128*, 11740–11741. (b) Hamaed, A.; Trudeau, M.; Antonelli, D. M. *J. Am. Chem. Soc.* **2008**, *130*, 6992–6999. (c) Hu, X.; Trudeau, M.; Antonelli, D. M. *Inorg. Chem.* **2008**, *47*, 2477–2484.
- (24) Kubas, G. J. *Proc. Natl. Acad. Sci. U.S.A.* **2007**, *104*, 6901–6907.
- (25) Lochan, R. C.; Head-Gordon, M. *Phys. Chem. Chem. Phys.* **2006**, *8*, 1357–1370.

JA809954R